Composition of carbonaceous fine particulate emissions of a flexible fuel DISI engine under high velocity and municipal conditions

Toni Miersch[a]

Hendryk Czech[a]

Benjamin Stengel[b, d]

Gülcin Abbaszade[c, d]

Jürgen Orasche[a, c]

Martin Sklorz[a, c]

Thorsten Streibel[a, c, d, *]

thorsten.streibel@uni-rostock.de

Ralf Zimmermann[a, c, d]

[a]Joint Mass Spectrometry Centre, Analytical Chemistry, Institute of Chemistry, University of Rostock, 18059 Rostock, Germany

[b]Piston Machines and Internal Combustion Engines, Faculty of Mechanical Engineering and Marine Technology, University of Rostock, 18059 Rostock, Germany

[c]Joint Mass Spectrometry Centre, Cooperation Group “Comprehensive Molecular Analytics”, Institute of Ecological Chemistry, Helmholtz Zentrum München – German Research Centre for Environmental Health, 85764 Neuherberg, Germany

[d]Helmholtz Virtual Institute of Complex Molecular Systems in Environmental Health (HICE), Germany

[*]Corresponding author at: Joint Mass Spectrometry Centre/Analytical Chemistry, Institute of Chemistry, University of Rostock, 18059 Rostock, Germany.

Abstract

A study about the chemical composition of carbonaceous fine particulate emissions of flexible fuel direct injection spark ignition engine under high velocity and municipal conditions was conducted with two different gasoline-ethanol blended fuels (E10 and E85). A self-designed engine test cycle simulating high vehicle velocity conditions of up to of 180 km/h was introduced (high velocity driving cycle, HVDC), simulating a possible motorway scenario without speed legislations as allowed in Germany, and compared to a municipal driving cycle (MDC), which is derived from the New European Driving Cycle (NEDC). The fingerprint of polycyclic aromatic hydrocarbons (PAHs) and their alkylated and oxygenated derivatives as well as the concentrations for PM2.5, elemental carbon (EC), organic carbon (OC) and also for the three most abundant PAHs were determined using a modified thermal optical carbon analyser (TOCA) hyphenated to soft resonance-enhanced multi-photon ionisation mass spectrometry (REMPI-TOFMS). Driving under high velocity conditions resulted in a significant increase of concentrations for PM, EC, OC, methyl-phenanthrenes and pyrene. Engine operation on E85 led to a strong decrease for all concentrations for both cycles. A good correlation was found between concentrations obtained by REMPI-TOFMS and TD-GC/MS. Most prominent PAHs were the alkylated series of phenanthrene, pyrene and naphthalene, whereby the abundances decrease with increasing degree of alkylation. The organic composition between HVDC and MDC mainly differed in quantity and to a lower extent in the aromatic pattern. Nevertheless, methyl-phenanthrenes, pyrene and methyl-pyrenes as well as 4H-cyclopenta[def]phenanthrene and benzo[b]naphtho[1,2-d]furan/benzo[b]naphtho[2,3-d]furan and it alkylated series showed a higher abundance in the pattern under high velocity conditions, where alkylated naphthalenes were enhanced in the MDC mode.

Keywords: Photoionization; REMPI; PAH; Gasoline-ethanol blend; Soot; Thermal optical carbon analysis

1 Introduction

In recent years, a growing demand for passenger cars could be observed worldwide. In 2017, 3.44 Mio new cars were registered in Germany alone, which denotes the highest amount in Europe and the fourth-largest worldwide with an still increasing trend [1,2]. Strict regulations have been introduced to decrease the emissions of greenhouse gases such as CO_2 and other regulated pollutants emitted by cars with diesel and gasoline engines, thus vehicle manufactures are forced to react to meet the legislation requirements. Although the proportion of cars with alternative powertrains (e.g. electric, hybrid) shows an increasing trend, cars with diesel or gasoline engine still dominate the sales figures in 2017, accounting for 40.3% and 56.5% of new registered cars in Germany, respectively [3]. The installation of diesel particulate filters (DPF) and selective catalytic reduction systems (SCR) ensure that modern diesel cars may fulfil new restrictions with respect to particulate matter (PM) and nitrogen oxide (NOx) emissions. Due to the introduction of direct injection (DI) and turbochargers in gasoline engines, their efficiency could be significantly enhanced, resulting in lower fuel consumption, possible engine down-sizing and associated decreased emission factors (EFs) for most regulated and unregulated pollutants. The drawback of the DI technique consists in significantly increased PM emission in contrast to the conventional port fuel injection (PFI) systems. Gasoline PM emissions may even exceed those of diesel engines equipped with DPF [4–7]. As a consequence, PM emissions of DI gasoline vehicles were limited to 5 mg/km (Euro 5 and Euro 6 standard) and 3 mg/mile in the USA (EPA Tier III standard). Cell exposure studies by Bisig et al. (2015) showed that the reduction of the particulate phase in spark ignition (SI) cars' exhaust by a gasoline particle filter (GPF) diminishes its genotoxicity [8]. Another possible strategy to reduce the particulate emissions of spark ignition engines (SI) is the operation with bio fuels such as bioethanol, which may also reduce the carbon footprint and carbon monoxide (CO) emissions [6]. So-called flexible-fuel-vehicles (FFV) can be operated on gasoline-ethanol blends up to 85% of ethanol, which are still a niche product in Germany, but claiming a big market share in Brazil [9]. The engine management of FFVs adjusts the time of fuel injection and ignition in dependence of the fuel ethanol content, resulting in optimized combustion conditions. Despite the fact that E5 (gasoline with maximum 5% ethanol content) refers to the most common fuel for gasoline engines in Germany, it can be expected that the consumption of E10 will increase within the general trend of biofuel addition to fossil fuels. Therefore it will be used in this study as fuel of the nearest future. E85 is also available in Germany, but covers a minor market share with 7,000 tons sold in 2015 [10]. Nevertheless, the E85 bio fuel is that with the highest ~~avaible~~available ethanol proportion and should demonstrate how strong emissions of state-of-the-art DISI FFV engines can be affected only by the switch to another fuel.

The soot reducing effect of ethanol was shown by several studies. Karavalakis et al. revealed that even 20% of ethanol may reduce PM significantly in a DISI engine [11,12], which was also reported earlier by Storey et al. and He et al. [13,14]. Hays et al. reported comparable results using a PFI engine [15]. Maricq et al. could observe a significant PM reducing effect of 30–45%, when the ethanol content exceeds 30% [16] and Clairotte et al. reported a decrease of 40% when switching from E5 to E85 [17].

However, not only the fuel composition and engine type have an impact on the emitted amount of pollutants. Emission legislations relate to a specific driving cycle with defined acceleration and deceleration phases and vehicle velocities. Until 2017, the New European Driving Cycle (NEDC) was performed as standard cycle for emission tests for new cars and should simulate the usual driving in urban and rural sites as well as motorways reaching a top vehicle velocity of 120 km/h [18]. This cycle was frequently criticised for not sufficiently covering realistic driving conditions, hence the worldwide harmonised light-duty vehicles test procedure (WLTP) will be used for emission certification of new vehicles beginning September 2018. Nevertheless, high velocities beyond 130 km/h which are allowed on German motorways are not covered by emission legislation test cycles. At higher velocities, the engine management of most gasoline cars switches to a fuel-rich mixture ($\lambda < 1$) to obtain higher engine power output and to avoid catalyst overheating, leading to a more incomplete combustion and elevated hydrocarbon and carbon monoxide emissions. The main scope of this work is to demonstrate how high velocity driving affects the emission of PM and its composition. For this purpose, a self-designed high velocity driving cycle (HVDC) was developed for engine tests simulating steady state car conditions with a maximum speed of 180 km/h. The four hour HVDC simulates a German long-distance travel scenario with an average velocity of 128 km/h, covering a start in urban environment, driving on a rural road, and afterwards high speed sequences between 120 km/h and 180 km/h. In contrast to the modified Common Artemis Driving Cycle (CADC, top velocity 150 km/h) the self-designed HVDC offers a less aggressive way of driving with an increased number of steady-state segments and less acceleration-and deceleration phases. Contrasting the high velocity driving, the second scenario reflected four-hour locomotion in an urban environment alone. The known and convenient acceleration, deceleration and velocity pattern from the NEDC cycle was taken as the basis for the cycle and continuously repeated with periods of idling in-between to avoid reiterative starting procedures. This driving pattern is referred as "municipal driving cycle" (MDC) for the purpose of this study and is also running for four hours. Both driving patterns were carried out with two fuels containing different contents of bioethanol, namely E10 and E85.

The released PM was analysed by a modified thermal-optical carbon analyser (TOCA), which is hyphenated to a soft resonance enhanced multiphoton ionisation time-of-flight mass spectrometer (REMPI-TOF-MS) [19,20]. This method allows a simultaneous determination of organic and elemental carbon (OC, EC) as well as the investigation of the aromatic fraction of particle-bound organic compounds. REMPI constitutes a very soft ionisation technique, which is both highly selective and sensitive to polycyclic aromatic hydrocarbons (PAHs). PAHs are mainly formed by incomplete combustion or pyrosynthesis at high temperatures under oxygen deficiency and are related to adverse health effects. That mass spectrometric approach was already applied for real-time characterisation of volatile as well as intermediate-volatile PAH emissions from combustion engines of light-duty passenger cars and heavy-duty vehicles [21,22]. The three major abundant compounds phenanthrene, methyl-phenanthrene(s) and pyrene will be quantified using an external calibration approach.

2 Methods and material

2.1 Engine

A 2.0L direct injection spark ignition (DISI) flexible fuel gasoline engine, equipped with a turbo charger and applied for Euro 5 emission standards, was operated on a test bench. For detailed engine specifications see Table S1 in the Supplemental Material. This DISI engine offers compatibility and optimized engine management for gasoline fuel with variable ethanol content ranging from 0 vol-% to 85 vol-%. The exhaust system was equipped with a three-way-catalyst (TWC) to convert carbon monoxide, nitrogen oxides and unburned hydrocarbons to carbon dioxide, nitrogen and water, respectively. An electric eddy current dynamometer (Schenck WM 400, Schenck RoTec GmbH, Darmstadt, Germany) was coupled to the engine's crankshaft and controlled by an LabVIEW® based software, which also acquired all relevant engine operations and data (diverse temperatures, pressures, torque, rotational speed, mass flows etc.) as well as the concentrations of all main combustion gases (CO, NOx, CO_2 and non-methane hydrocarbons (NMHC). Gas concentrations were determined by Fourier transform infrared spectroscopy (AVL SESAM i60 FT, AVL List GmbH, Graz, Austria), sampling from the tail-pipe after the TWC. Synthetic long life 5W30 oil (Formula VX Long Life, Q8 Oils, Kuwait Petroleum Corporation) was used as lubricant, which was substituted after half of the experiments (100 operating hours) had been performed. The engine was operated using patterns for speed and torque based on engine conditions in a mid-sized passenger vehicle.

2.2 Fuels

The engine was operated on two commercial fuels with different ethanol content: gasoline with 5.19%-vol ethanol (DIN EN 228, TEAM Mineralöle GmbH) and gasoline with 83.13%-vol ethanol (DIN 51625, Vorwerk Mineralöl GmbH), named here E10 and E85 respectively. For detailed properties of the tested fuels see Table S2.

2.3 Driving cycles

Two self-designed driving cycles, the high velocity driving cycle (HVDC) and the municipal driving cycle (MDC) were performed in this study. The fundamental patterns for both cycles are illustrated in Fig. 1. The MDC cycle consisted of eleven parts based on the velocity pattern of the New European Driving Cycle (NEDC). It started with one cold start cycle (room temperature ~20 °C). Afterwards it was repeated ten times without engine shutdown and restarts in between, however each single cycle was extended by 40 s of idling. The whole cycle ended with 980 s of idling, resulting in four hours of driving and sampling time, equalling 121.25 km.

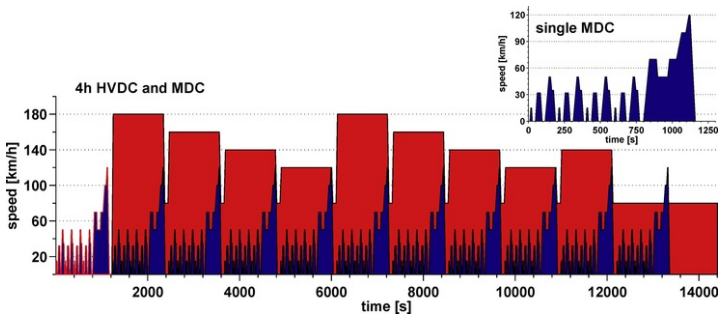

Fig. 1 Used driving cycles; red) High Velocity Driving Cycle (HVDC) and blue) Municipal Driving Cycle (MDC).

The HVDC was also divided into eleven parts, beginning as well with one cold start MDC followed by four sequences, which were executed twice. Each sequence consisted of 1220 s of driving with maximum speeds of 180, 160, 140 or 120 km/h, with short 80 km/h phases in between. The cycle was accomplished with 1220 s of 140 km/h and 2200 s of 80 km/h, resulting as well in four hours of driving and sampling time, equalling 511.20 km.

2.4 PM sampling

The raw exhaust from the engine was diluted by a porous tube diluter followed by an ejector diluter (VC-DAS, Venacontra, Kuopio, Finland) to an average dilution ratio of ~10. For chemical analysis fine particulate matter with an aerodynamic diameter below 2.5 µm was collected with a modified speciation sampler equipped with a PM2.5 impactor (Rupprecht & Patashnik 2300, Thermo Scientific, Waltham, USA) on 47 mm quartz fibre filters (QFF, T293, Munktell, Sweden) at a flow rate of 10 L/min, resulting in a sampling volume of 2.4 m^3 over four hours. The QFFs were preconditioned 12 h at 550 °C and stored in sealed glass containers. Directly after sampling, filters were frozen at −25 °C and stored at this temperature till analysis. To determine the PM weight, PTFE filters were used for sampling and were weighted before and after sampling using a micro balance.

2.5 Instrumental setup

For analysis of the carbonaceous fraction of PM, a modified thermal-optical carbon analyser (TOCA, Modell 2001A, DRI, Reno, USA), which is hyphenated to a soft photo-ionisation time-of-flight mass spectrometer, was utilised (Fig. 2). A detailed description of the setup can be found elsewhere [19]. This technique enables the simultaneous characterisation of the aromatic composition of organic matter and the determination of organic and elemental carbon (OC, EC). Each sample was analysed in triplicate and found to be within the given instrumental precision of 2–6%, whereby one sample denotes a circular filter punch of 0.5 cm^2 from the original filter. The carbon analysis was carried

out according to the Improve-A protocol [23]. Organic material evolves during four thermal fractions (OC1, OC2, OC3 and OC4) in helium atmosphere at temperatures of 140, 280, 480, and 580 °C, respectively. By adding 2% of oxygen to the helium atmosphere, elemental carbon is oxidised to CO_2 in three EC fractions (EC1, EC2, EC3) at 580, 740 and 840 °C, respectively. For the optical correction of pyrolytic OC, laser transmittance at 635 nm was preferred over laser reflectance because of relatively low filter loads. The analysers original quartz cross was modified with an extension of a small heated quartz arm between sample oven and oxygenator, with which a minor part (approximately 2 ml/min) of the sample flow is transferred from the carbon analyser through a heated deactivated fused silica capillary (I.D. 200 µm) to the vacuum ion source of the mass spectrometer. Subsequently, ionisation is carried out by resonance enhanced multiphoton ionisation (REMPI) with 266 nm photons provided by the fourth harmonic of a pulsed Nd:YAG laser (Big Sky Ultra, Quantel, Les Ulis, France) with a repetition rate of 20 Hz. In this two-step ionisation process ([1 + 1]-REMPI) low fragmentation and high selectivity towards (poly)aromatic compounds are achieved with low limits of detection depending on the absorptivity and lifetime of the intermediate excited electronic state [24]. Ions were separated according to their mass to charge ratio (m/z) by a reflectron time-of-flight mass spectrometer (CTF 10, Stefan Kaesdorf, Munich, Germany), which provides a mass resolution of ~650 at m/z 112 [25]. During data acquisition, 20 consecutive spectra were averaged to reduce the signal-to-noise ratio yielding in a time resolution of 1 s. All spectra recorded for each thermal fraction were summed up. Obtained signals were normalised to the intensity of 1 ppm toluene standard gas (Linde AG, Germany), which was daily analysed, to compensate for minor fluctuations of laser energy.

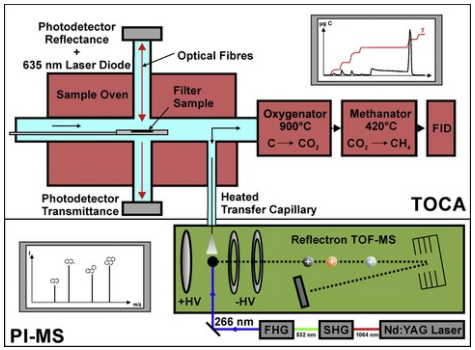

Fig. 2 Instrumental Setup; TOCA hyphenated to REMPI-TOF-MS, frequency multiplication of fundamental laser wavelength of 1.064 nm by second harmonic generation (SHG) and fourth harmonic generation (FHG) to target wavelength of 266 nm.

2.6 PAH quantification

The quantification of phenanthrene, methyl-phenanthrenes (as sum of all five isomers) and pyrene was conducted by external calibration on the basis of DIN 38402-53. Studies of Munoz et al. (2016) showed that 3-methyl-phenanthrene is the most abundant methyl-phenanthrene isomer on gasoline soot thus this isomer was used as standard for all isomers [26]. For this purpose, a serial dilution consisting of eight equidistant and independently prepared concentrations was prepared in n-hexane as solvent, which evaporates rapidly and is not ionised by REMPI. From each calibration standard 5 µl was pipetted on a pre-heated quartz fibre filter punch. After 30 s of drying at ambient air, the filter was placed into the carbon analyser and measured according to the Improve-A protocol, whereby each filter load was measured in triplicate. Only m/z-of 178, 192 and 202 in the OC1 and OC2 fraction were considered and summed up over the duration of both OC fractions. The linear fit function with corresponding confidence interval at a significance level of 95% and the limit of detection (LOD), the limit of quantification (LOQ), the residual standard deviation (s_y) and the coefficient of determination (R^2) for each component can be found in the supplement in Table S3 and Fig. S4. All signals were also normalized to 1 ppm toluene signal, in the same manner as explained in the previous section. The obtained concentrations are compared with those obtained from thermodesorption gas chromatography-mass spectrometry (TD-GC/MS) which constitutes an established reference technique [27]. With TD-GC/MS the organic fraction of PM can be analysed directly from the filter and without any further sample preparation. Therefore, TD-GC/MS as a direct analysis technique is well-suited as a reference technique for TOCA-REMPI-TOFMS.

3 Results and discussion

3.1 Regulated emissions

The mean fuel consumption in E10 experiments was 9.63 kg/h and 2.20 kg/h, for HVDC and MDC, respectively, which is equivalent to 10.69 L/100 km and 9.91 L/100 km. The lower heating value of E85 (33.13 MJ/kg, compared to 42.51 MJ/kg for E10) resulted in an increased fuel consumption for both E85 experiments with 13.96 kg/h and 3.13 kg/h for HVDC and MDC, respectively, which is equivalent to 13.94 L/100 km and 13.14 L/100 km. The differences in fuel consumption (per 100 equivalent kilometres) between both cycles were surprisingly low because the motor efficiency (mechanical energy output/fuel energy input) is reduced at low engine loads, dominating in MDC (E10: 25.7% and E85: 23.4% in mean) and enhanced at high loads, dominating in HVDC (E10: 34.4% and E85: 31.5% in mean). Moreover, the higher frequency of acceleration- and deceleration phases lead to increased fuel consumption in MDC mode, while high velocity driving is composed of more steady state segments and less speed changing sections.

Concentrations and emission factors of inorganic gaseous emissions (NOx, CO) and organic pollutants (NMHC) are summarised in Table 1. An enhanced CO concentration during high velocity conditions is the consequence of a low air/fuel mixture ($\lambda < 1$), which is needed to obtain high engine loads and avoid overheating. The TWC cannot completely reduce the CO, because of insufficient oxygen supply, which was also observed by Fontaras et al. in the Artemis Motorway Cycle at higher speeds [7]. By using E85 fuel, the increased fuel oxygen content lead to a more complete combustion and lowered CO concentrations. NOx emissions were elevated during high velocity conditions and emitted in equal concentrations independently from the ethanol content of the fuel. The mean PM2.5 concentration was increased by 32% for HVDC compared to MDC with the use of E10 and was reduced by 88% in HVDC and 80% in MDC by switching from E10 to E85.

Table 1 Mean concentrations after TW NOx, CO, NMHC, PM 2.5, EC and OC in ppm and mg/m^3 and emission factors for NOx, CO, NMHC in mg/kg fuel and respective conversion factors to mg/kWh.

	E10 HVDC			E10 MDC			E85 HVDC[d]			E85 MDC		
	ppm	mg/m^3	mg/kg fuel	ppm	mg/m^3	mg/kg fuel	ppm	mg/m^3	mg/kg fuel	ppm	mg/m^3	mg/kg fuel
NOx[a]	5.97 (1.64)	8.00 (2.20)	61.25 (17.53)	3.88 (1.86)	5.20 (2.50)	19.54 (11.24)	5.79 (0.94)	7.76 (1.26)	27.80 (5.34)	4.18 (0.73)	5.60 (0.95)	16.27 (3.34)
CO	2077 (505)	2596 (631)	64,300 (18466)	307 (138)	384 (173)	1210 (700)	493 (1.85)	616 (2.31)	9546 (56)	84 (65.40)	150 (81.75)	258 (197)
NMHC[b]	10.50 (1.26)	7.50 (0.90)	31.93 (22.02)	11.56 (1.64)	8.26 (1.17)	39.59 (6.08)	16.89 (8.37)	12.07 (5.98)	53.75 (36.61)	140.23 (53.87)	100.16 (38.48)	195.88 (195.35)
PM 2.5	–	2.93 (0.21)	–	–	2.22 (0.55)	–	–	0.35 (0.21)	–	–	0.44 (0.18)	–
EC	–	2.67 (0.22)	–	–	1.61 (0.13)	–	–	0.10 (0.06)	–	–	0.07 (0.01)	–
OC	–	0.30 (0.02)	–	–	0.22 (0.03)	–	–	0.14 (0.04)	–	–	0.12 (0.03)	–
Conversion factor to mg/kWh[c]	–	–	0.2461	–	–	0.3296	–	–	0.3452	–	–	0.4645

[a] NOx in NO equivalents.

[b] NMHC in methane equivalents.

[c] Conversion factor from mg/kg fuel to mg/kWh.

[d] Two experimental replicates; values in brackets refer to standard deviation.

3.2 EC and OC emissions

The fraction of OC which is volatilised below 280 °C (OC1 + OC2) accounts for ~60% of detected organic carbon, whereas OC3 and OC4 represents approximately 30% and 10%, respectively, in all experiments. Roughly half of the available elemental carbon was detected in EC1 with a first flat and later slowly declining FID signal, followed by a sharp peak in EC2 explaining the remaining EC. These peak shapes were also reported by Watson et al. [28].

Both E10 experiments show low OC-EC-ratios with 0.11 and 0.13 for HVDC and MDC, respectively. These low ratios can be attributed to the removal of hydrocarbons by the three-way-catalyst while EC emissions are retained. This agrees with the results of Storey et al. (2010) who demonstrated that EC is not expected to be affected by the three-way-catalyst due to too short residence times in the catalytic converter [13]. Driving in high velocity mode resulted in 41% higher concentrations for OC ($p = 3.3E-4$) and 66% higher concentrations for EC ($p = 5.1E-6$), which can be explained by the increased fuel consumption and the non-stoichiometric combustion in HVDC. Results of Fushimi et al. (2016) and Hays et al. (2013) also show that EC is the main contributor to total carbon (TC), which is in turn the main constituent of gasoline particulate matter (E10) [15,29].

When the engine was operated with E85, the OC-EC-ratios increased to 1.33 and 1.69 for HVDC and MDC, respectively. The increased oxygen content in the E85 fuel (29.00%-wt vs. 2.64%-wt in E10) leads to a more complete combustion and consequently to decreased EC emissions. In flame studies of Wu et al. (2006) it was shown that oxygenates such as ethanol may have an impact on soot formation due to the limitation of aromatic precursors [30]. Hays et al. (2013) also reported an increased OC-EC-ratio by using higher oxygenated fuels [15]. EC emission was decreased roughly by 2 orders of magnitude and OC by the factor of 2. However, significant differences cannot be observed for OC or EC between the two driving cycles in E85 experiments, which may have several reasons. First of all, the engine management system can take advantage of the higher octane number of E85 and shift the switch to a rich fuel-air-mixture towards even higher loads leading to an enhanced TWC efficiency compared to E10 operation. Furthermore, it should be mentioned that in the case of E85 samples very low filter loadings were obtained (total carbon: 1–3 µg C/cm^2), which are in the lower range of the instrument's quantification limits and thus are subjected to an increased error. Nevertheless, by operating the FFV engine with E85 fuel, the emission of carbonaceous aerosol is reduced significantly, independent of the driving cycle.

Although MDC was closely related to NEDC, it should be noted that the test-bench could not follow perfectly the desired patterns for engine speed and torque especially when the desired engine torque was negative (engine brake) due to its eddy current dynamometer. Therefore, results for engine emissions of all investigated emissions and fuel consumption are not comparable to results from chassis dynamometer tests.

3.3 Emissions of semi-volatile aromatic compounds

Resonance-enhanced multi-photon ionisation is a powerful tool to gain insights into the molecular composition of organic carbon, especially to the aromatic fraction. As previously shown [19], mainly semi-volatile species were expected in the first two OC-steps (up to 280 °C) followed by decomposition products of larger, low- to non-volatile substances in the subsequent temperature step (T = 280–480 °C). The last OC fraction (OC4, T = 480–580 °C) did not provide any abundant signals in MS, thus OC4 will not be discussed in the following. Mass spectra of OC1 and OC2 were summed up and will be referred as “semi-volatile fraction”. Fig. 3 visualises the obtained REMPI mass spectra of the four experiment types. The semi-volatile fractions of E10 samples are dominated by polycyclic aromatic hydrocarbons (PAHs) and their homologues alkylation series, whereby the most abundant species corresponds to alkylated phenanthrenes (*m*/*z* 178, 192, 206, 220, 234) and alkylated pyrenes (*m*/*z* 202, 216, 230) up to C4-substitution. Intensities above SNR = 3 were observed in the *m*/*z* range from 94 to 252 corresponding to phenol and benzo-pyrenes/benzo-fluoranthenes, respectively. Altogether, absolute intensities differ by the factor of two in favour of HVDC. The most intense signal of each homologue series belongs to the parent PAH or PAH-derivatives followed by the alkylated species with inverse correlation between alkylation and intensity. In both scenarios, HVDC and MDC, phenanthrene (*m*/*z* 178) provides the most abundant signal, followed by pyrene (*m*/*z* 202). Single species identification made here is only possible due to different REMPI ionisation cross sections of isobaric compounds at the used photon energy. At 266 nm, the cross section of the phenanthrene isobaric compound anthracene is negligible, hence *m*/*z* 178 was solely assigned to phenanthrene [19,31]. However, the applied method cannot distinguish between different isomers with the same degree of alkylation because with growing PAH core structure the position of alkylation has a progressively smaller effect on the cross section at the specific wavelength. In addition, the absolute peak heights do not reflect the absolute sample composition because cross sections of different species may differ up to two orders of magnitude [21,31].

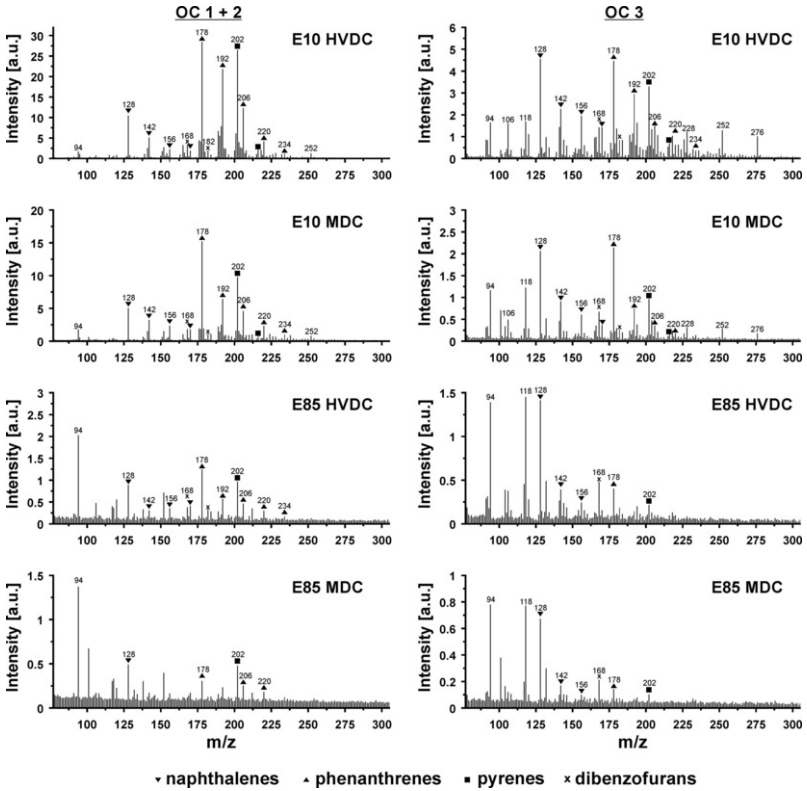

Fig. 3 REMPI mass spectra for all experimental conditions left) summed up spectra for the semi-volatile fractions (OC 1 + OC 2) and right) OC 3 fraction. The most prominent alkylated series are indicated.

As described in the previous section, oxygenates such as ethanol exhibit a soot reducing effect in combustion processes due to the limitation of aromatic precursors [30]. The production of OH radicals out of ethanol plays an important role by removing reactive hydrogen atoms, which may reactivate relatively stable aromatic molecules and can promote the ring growth process towards soot by addition of acetylene molecules (HACA mechanism, H-Abstraction-C_2H_2-addition) [32]. Therefore, the semi-volatile fraction of E85 reveals low abundant signals compared to E10 samples, in both HVDC and MDC. For example, phenanthrene is less abundant on the E85 particulate emissions by the factor of 22, while pyrene even shows a 26-fold diminished response (HVDC). This reduction implicates that particle-bound PAHs can be lowered significantly by engine operation on the highest possible ethanol amount. Furthermore, it can be assumed, that particle-bound PAHs primarily originate from the incomplete combustion of the fossil components in the respective, which are 5.7-times higher concentrated in E10 than in E85. This suggests, that ethanol has not only a “diluting”-effect, but also play an active role in the gasoline combustion chemistry.

The pattern of the decomposed fraction (OC3) shows similarities to that of the semi-volatile one (OC1 + OC2). Particulate semi-volatiles from diesel engines may originate from unburned fuel and have strong chemical resemblances with the used fuel [33]. E10 as well as E85 are very volatile fuels and only contain minor amounts of semi-volatile compounds that are expected to appear in the particle phase. In conclusion, it can be assumed that most species detected in OC1 and OC2 were formed by pyrosynthesis during combustion, which is in accordance with the observed typical pattern of decreasing abundances with increasing alkylation, also observed in previous findings [29]. In OC3, the shift towards smaller m/z is caused by the pyrolysis of high-molecular-weight substances, which decompose before evaporation. The most abundant signals correspond to polycyclic aromatic degradation products, such as naphthalene (m/z 128), phenanthrene (m/z 178), pyrene (m/z 202), benzopyrene (m/z 252), benzo[ghi]perylene/indeno[1,2,3-cd]pyrene (m/z 276) and smaller thermal degradation products, e.g. phenol (m/z 94) and indane/benzofuran (m/z 118). The alkylation distribution is in agreement with the pattern of the semi-volatile fraction. Generally, the intensities in OC3 mass spectra were reduced in comparison to the mass spectra of the semi-volatile fraction (E10). There are no clear differences in pattern of OC3 between HVDC and MDC with E10 fuel, but intensities are diminished analogous to the semi-volatile fraction. The low-volatile fraction of E85 particulate matter shows a similar pattern without significant differences between HVDC and MDC, but with strongly attenuated abundances compared to E10.

Particle-bound PAHs mainly differ in concentration, but to a lower extent in their alkylation patterns. Minor changes in the distribution of these compounds may not be noticeable on first view, thus a two-sample t-test was carried out to reveal significant differences in the pattern. Intensities in E85 mass spectra are low and near the limit of detection and therefore only E10 data were subjected to the t-test. The necessary conditions for the accomplishment of a t-test are that 1) the two data sets are independent of each other 2) the respective data sets are normal distributed and 3) have equal variances (variance homogeneity). All statistical tests were carried out in Matlab 7.11 (R2010b) at a significance level of $\alpha = 0.05$. The three instrumental replicates of each sample were averaged, which results in six and five mass spectra for HVDC and MDC, respectively. Only even m/z between 78 and 350 providing $S/N \geq 6$ were considered for the following tests. To highlight the differences in the alkylation pattern and not the quantitative distinctions, the mass spectra were normalised to the base peak (BP). It was waived for a test for normal distribution, due to the little sample size and the robustness of t-test for non-normal distribution [34]. A two-sided Grubbs outlier test was performed for each m/z in the respective value set and detected outliers were removed. A subsequent F-test identified m/z that were not variance homogeneous in both populations and subjected them to a Welch’s t-test, which is more robust in this scenario. The remaining values that were showing variance homogeneity were evaluated with Student’s t-test.

In Fig. 4, the results of the statistical pattern comparison between HVDC and MDC are illustrated in a volcano diagram. The fold change (FC) on the x-axis presents a quantitative measure while the p-value on the y-axis indicates statistical significance. Mass over charge ratios that are considered as significantly different by means of p-values < 0.05 are exclusively pronounced for HVDC except m/z 212, which is 106% higher in MDC patterns and can be attributed to C6- naphthalene. Furthermore C2- to C4-naphthalenes (m/z 156, 170, 184) are enriched in MDC patterns as well with 86%, 124% and 238%, respectively. Species that are significantly more abundant in HVDC patterns are linked to methyl-phenanthrenes (m/z192), pyrene (m/z202) and methyl-pyrenes (m/z216), which are enriched by 46%, 24% and 64%, respectively. Compounds with m/z of 176, 190, 218 and 232 have also higher abundances in the HVDC. Possible compounds that could be linked to the detected m/z are high alkylated benzenes with C7- to C-11 alkylation, but also 4H-cyclopenta[def]phenanthrene (m/z 190) or benzo[b]naphtho[1,2-d]furan / benzo[b]naphtho[2,3-d]furan (m/z 218) and their alkylation series, which were also reported to be present in gasoline and diesel soot [35,36]. A possible source of the latter compounds is thermal degradation of the lubrication oil, which can make up to 20% of the particulate emissions of a DISI engine, but recombination and pyrolysis products of the used fuel or a combination of both are also plausible [29,37]. In conclusion, two-ring PAHs are found to be more present in the pattern of MDC experiments, whereby three-and four-ring PAHs are more abundant under HVDC conditions. The operation under high velocity conditions led to increased temperatures in the engine combustion zone and exhaust system as well as to a lack of oxygen. These conditions could promote the evaporation and degradation of minor amounts of lubrication oil and also initiate other processes than during MDC conditions. Nevertheless, the absolute intensities of such compounds are relatively small and do not provide a major part of the total detected compounds.

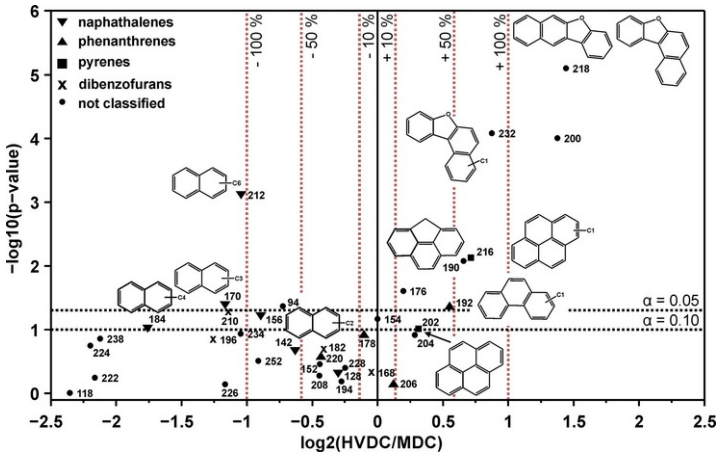

Fig. 4 Volcano plot comparing pattern of the semi-volatile fraction of HVDC with MDC of the E10 experiments. X-axis shows the fold change and y-axis the significance level. Each data point is linked to one *m/z* ratio. Horizontal black dashed lines refers to a significance level of 5% and 10% and vertical red dashed lines refer to a fold change of 1.1 and 1.1^{-1}, 1.5 and 1.5^{-1}, 2 and 2^{-1}. Alkylated series are indicated and possible structures are given.

3.4 Quantification of major aromatic semi-volatile organic compounds

Adam et al. (2012) already described that REMPI-TOF-MS is a robust tool for semi-quantification of monocyclic and polycyclic aromatic hydrocarbons for chassis dynamometer testing [21]. Semi-quantification in that study was based on the photo-ionisation cross sections of the analytes relative to a calibrated compound (e.g. toluene). This requires a continuous standard gas flow, which is not feasible in the experimental setup used in this study and so an external calibration approach was conducted to quantify particle-bound organic species with REMPI-TOF-MS. Previous TD-GC/MS measurements of the same samples suggests that phenanthrene, methyl-phenanthrene (as sum of all five isomers) and pyrene are the most abundant polyaromatic compounds on gasoline soot particles, which is in accordance with the results of Munoz et al. [26]. These compounds deliver a good base for quantification with REMPI-TOF-MS, due to their low limit of detection (LOD), the availability of standards, a relative clear assignment to a specific *m/z* and a high disposability on gasoline soot. Particle bound aromatic compounds from the operation with E85 were only present in minor amounts and showed intensities below the limit of quantification and the limit of detection. Due to the instrumental design it is not possible to increase the sample amount (e.g. the filter punch size) that can be analysed in a single run, hence quantified values for E85 are not discussed.

The obtained concentrations of the investigated compounds are illustrated in Fig. 5 and can also be found in Table S5. Independent from the driving cycle, phenanthrene denotes the most abundant detected PAH on gasoline particulate emissions. On average 636 ng/m^3 phenanthrene is emitted in the E10 high velocity experiment, whereas the more passive driving in MDC emits 484 ng/m^3. In the case of phenanthrene concentrations a high standard deviation was observed, whereby a *t*-test revealed that the phenanthrene concentration does not differ significantly between the driving cycles ($p = 0.2$). Methyl-phenanthrenes are increased by 150% from 222 ng/m^3 in MDC to 554 ng/m^3 in HVDC on average. In contrast to phenanthrene, the scattering of determined values between single engine runs was lower, so the mean difference between HVDC and MDC with E10 fuel is statistically significant ($p = 9.3E-7$). Pyrene was emitted in a similar quantity as the methyl-phenanthrenes at increased engine loads with 566 ng/m^3 and was reduced significantly by a factor of two during MDC to 309 ng/m^3 ($p = 4.3E-4$).

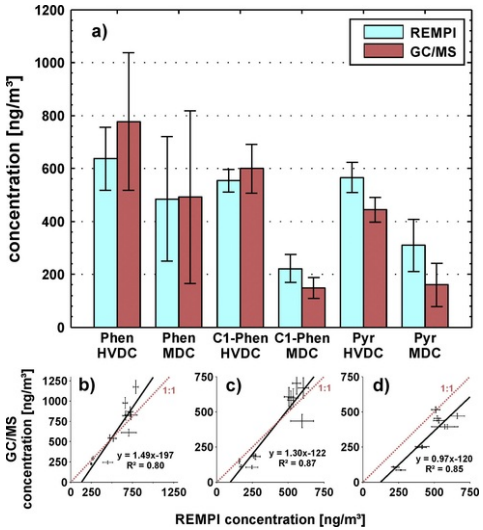

Fig. 5 (a) Mean concentrations for phenanthrene, methyl-phenanthrenes (C1-phenanthrenes) and pyrene in E10 experiments determined by REMPI-TOF-MS (blue) and TD-GC/MS (red) in ng/m^3. Error bars refer to standard deviation. Lower Panels: single concentrations obtained from REMPI-TOF-MS plotted vs. TD-GC/MS for (b) phenanthrene, (c) C1-phenanthrenes and (d) pyrene; error bars show coefficient of variation, black solid lines show linear fit and red dashed lines the theoretical 1:1 curve progression. (For interpretation of the references to colour in this figure legend, the reader is referred to the web version of this article.)

By using E85, the estimated concentrations were decreased for each of the investigated compounds and driving cycles, but without significant differences of the mean concentrations between the cycles. The E10 results were compared with TD-GC/MS measurements of the same samples, which are additionally depicted in Fig. 5a) and are found to be in good agreement. Furthermore in Fig. 5b, c, d) raw exhaust concentrations of REMPI-MS and TD-GC/MS are plotted against each other and a good correlation between both methods can be found for all three compounds. Generally, the determined concentrations for E10 obtained with the REMPI method differ by a factor of 1.3 on average from that determined by TD-GC/MS. However, TOCA-REMPI-TOFMS can provide information about the distribution between the OC1 and OC2 fraction, i.e. how strong a compound is bound to the particles. This reflects the position of the gas-particle equilibrium thus in principle atmospheric implications could be drawn [38]. The time traces of the three selected compounds over the OC fractions are illustrated in Fig. S9 for both E10 experiments. For instance, pyrene showed a significant different distribution between both fractions depending on the driving cycle ($p = 1.4E-3$). In HVDC 36.1% of the pyrene is evolved in OC1 and 63.9% in OC2, whereas in MDC 45.6% is desorbed in OC1 and 54.4% in OC2. Methyl-phenanthrenes on particles derived from high velocity conditions are evaporated to 56.2% in OC1 and to 43.8% in OC2, whereas MDC particles show a significant different behaviour with 62.5% in OC1 and 37.5% in OC2 ($p = 2.1E-4$). Slightly more phenanthrene is desorbed in OC1 in both cycles (56.0% and 57.6%) compared to OC2 (44.0% and 42.4%), but without significant differences of the means for MDC and HVDC ($p = 0.17$). In comparison, during the external calibration process the investigated species were nearly completely evaporated in OC1 and only a minor amount could be detected in OC2. The way of driving seems to have an effect not only on the PM emission, but as well on the particle morphology. Organic matter originating from HVDC conditions appears to be stronger attached to the particle's elemental carbon core structure, leading to an increase of the desorption temperature. The partitioning of PAHs between different fractions of OC might have relevance on the participation either in homogenous or heterogeneous reactions with atmospheric oxidising agents, such as OH radicals or ozone. Such reactions can progress with different reactivity and consequently different contribution to either secondary organic aerosol (SOA) or aged primary organic aerosol (aged POA) [39].

Generally, driving under high velocity conditions led to increased emissions, which can be explained by increased fuel consumption and a non-stoichiometric combustion (fuel-rich mixture) at higher loads. The effect was expected to be more pronounced, but engine efficiency under urban conditions (~24%) with many acceleration and deceleration phases is strongly reduced compared to higher loads and more steady state sequences (~34%). The results of Munoz et al. (2016) have shown that driving with a DISI engine at constant loads and moderate velocities reduces emission factors of all regulated and unregulated pollutants as well as fuel consumption dramatically [26], which seems to play a role at high velocities as well.

4 Conclusion

The study investigated how high velocity driving conditions affect the emission and composition of fine particulate matter of a DISI engine operated on gasoline with an ethanol content of 5% and 85% (E10 and E85), respectively. To cover high velocity conditions, a self-designed high velocity driving cycle simulating vehicle top speeds up to 180 km/h was introduced, which was compared to the MDC cycle, reflecting urban traffic conditions. Driving

under HVDC conditions with E10 fuel yielded in increased CO concentrations, due to a fuel-rich combustion and consequently reduced TWC efficiency. CO concentrations were significantly decreased in both cycles by the use of E85. High velocity conditions released 32% higher concentrated PM emissions than MDC conditions while the usage of E85 lowered particulate concentrations significantly by 88% and 80% for both cycles, respectively. It could be observed that total carbon accounted for almost 100% of the emitted particulate material, whereby the OC/EC ratio is strongly affected by the used fuel. Operation on E10 yielded in OC/EC of 0.11 and 0.14 and for E85 1.35 and 1.71 for HVDC and MDC, respectively. Low ratios can be assigned to the removal of organic compounds in the exhaust by the TWC, which does not affect EC emissions. Higher fuel ethanol content led to a more complete combustion resulting in lower EC emissions due to the increased oxygen content, the limitation of aromatic precursors and consequently an increase of OC-EC ratio. Main aromatic constituents were the alkylated series of phenanthrene and pyrene, but the homologue series of naphthalene could be observed as well. The parent PAH always represented the highest abundance of a homologue series. With increasing degree of alkylation the intensities decreased which indicates that these compounds were formed by pyrosynthesis during the combustion process and did not originates from unburned fuel. Particle bound PAHs mainly differed by their concentrations, but only to a lower extent in the aromatic pattern. A *t*-test revealed that alkylated naphthalenes were slightly enhanced in the MDC mode, whereby 4H-cyclopenta[def]phenanthrene and benzo[b]naphtho[1,2-d]furan/benzo[b]naphtho[2,3-d]furan and their alkylated derivatives along with pyrene, methyl-pyrenes and methyl-phenanthrenes were enriched during HVDC. Mass concentrations obtained by external calibration showed that all methyl-phenanthrenes and pyrene were significantly increased during high velocity conditions, whereby concentrations for phenanthrene were not found to be significantly different between the driving cycles. Furthermore, the use of E85 led to strongly attenuated concentrations for PAHs, which appeared below the limit of quantification for all quantified analytes. The comparison with quantified values determined by TD-GC/MS demonstrated that the external calibration approach using TOCA-REMPI-TOF-MS provides similar results with additional information about the adsorptivity of the particle-bound PAHs and thus the participation in homogenous or heterogeneous atmospheric reactions after gas-particle equilibrium.

For a more comprehensive assessment of the impact of gasoline exhaust on human health toxicological studies must be carried out. This goal was also targeted during the same measurement campaign by the exposure of lung cells with combustion aerosol using an air-liquid-interface [40,41]. The results of these biological experiments will be subjected to a future publication.

Conflict of interest

The authors declare that they have no conflict of interest.

Acknowledgement

This work was conducted at the Institute of Piston Machines and Internal Combustion Engines of the University of Rostock in cooperation with the Helmholtz Virtual Institute of Complex Molecular Systems in Environmental Health (HICE) and was funded by the Deutsche Forschungsgemeinschaft (DFG, grant ZI 764/7-1), the Helmholtz Impulse and network Funds of the Helmholtz Association (Germany) and the DACH-project WooShi (grant ZI 764/5-1). All funders are gratefully acknowledged. The authors thank also all technical assistants that were involved during the field campaign.

Appendix A. Supplementary data

Supplementary data to this article can be found online at https://doi.org/10.1016/j.fuel.2018.09.136.

References

[1] VDA. Neuzulassungen von Personenkraftwagen (Pkw) im Jahr 2017 nach Ländern (in Millionen): Statista. [September 18, 2018]; Available from: https://de.statista.com/statistik/daten/studie/181566/umfrage/neuzulassungen-von-personenkraftwagen-nach-laendern/.

[2] ACEA. Anzahl der Neuzulassungen von Pkw in einzelnen Ländern Europas im Jahr 2017: Statista. [September 18, 2018]; Available from: https://de.statista.com/statistik/daten/studie/36395/umfrage/anzahl-der-pkw-neuzulassungen-in-den-laendern-europas/.

[3] Center of Automotive Management. Anteil ausgewählter Kraftstoffarten an den Neuzulassungen von Personenkraftwagen in Deutschland im Zeitraum der Jahre 2010 bis 2017: Statista. [September 18, 2018]; Available from: https://de.statista.com/statistik/daten/studie/699301/umfrage/anteil-von-kraftstoffarten-an-neuzulassungen-von-pkw-in-deutschland/.

[4] B. Liang, Y. Ge, J. Tan, X. Han, L. Gao, L. Hao, et al., Comparison of PM emissions from a gasoline direct injected (GDI) vehicle and a port fuel injected (PFI) vehicle measured by electrical low pressure impactor (ELPI) with two fuels: gasoline and M15 methanol gasoline, *J Aerosol Sci* **57**, 2013, 22–31.

[5] J. Jang, J. Lee, J. Kim and S. Park, Comparisons of the nanoparticle emission characteristics between GDI and PFI vehicles, *J Nanopart Res* **17** (12), 2015.

[6] G. Karavalakis, D. Short, R.L. Russell, H. Jung, K.C. Johnson, A. Asa-Awuku, et al., Assessing the impacts of ethanol and isobutanol on gaseous and particulate emissions from flexible fuel vehicles, *Environ Sci Technol* **48**

(23), 2014, 14016–14024.

[7] G. Fontaras, V. Franco, P. Dilara, G. Martini and U. Manfredi, Development and review of Euro 5 passenger car emission factors based on experimental results over various driving cycles, *Sci Total Environ* **468–469**, 2014 1034–1042.

[8] C. Bisig, S. Steiner, P. Comte, J. Czerwinski, A. Mayer, A. Petri-Fink, et al., Biological effects in lung cells in vitro of exhaust aerosols from a gasoline passenger car with and without particle filter, *Emiss Control Sci Technol* **1** (3), 2015, 237–246.

[9] ANFAVEA. Verteilung des Fahrzeugabsatzes in Brasilien im Jahr 2015 nach Kraftstoffarten: Statista. [February 20, 2017]; Available from: https://de.statista.com/statistik/daten/studie/150370/umfrage/fahrzeugabsatz-nach-kraftstoffart-in-brasilien.

[10] FNR. Absatz von Bioethanol in Deutschland in den Jahren 2007 bis 2015 (in 1.000 Tonnen): Statista. [February 20, 2017]; Available from: https://de.statista.com/statistik/daten/studie/198583/umfrage/absatz-von-bioethanol-in-deutschland/.

[11] G. Karavalakis, D. Short, D. Vu, M. Villela, R. Russell, H. Jung, et al., Regulated emissions, air toxics, and particle emissions from SI-DI light-duty vehicles operating on different iso-butanol and ethanol blends, *SAE Int J Fuels Lubr* **7** (1), 2014, 183–199.

[12] G. Karavalakis, D. Short, D. Vu, M. Villela, A. Asa-Awuku and T.D. Durbin, Evaluating the regulated emissions, air toxics, ultrafine particles, and black carbon from SI-PFI and SI-DI vehicles operating on different ethanol and iso-butanol blends, *Fuel* **128**, 2014, 410–421.

[13] J.M. Storey, T. Barone, K. Norman and S. Lewis, Ethanol blend effects on direct injection spark-ignition gasoline vehicle particulate matter emissions, 2010, SAE International; Warrendale, PA.

[14] He X, Ireland JC, Zigler BT, Ratcliff MA, Knoll KE, Alleman TL et al. The impacts of mid-level biofuel content in gasoline on SIDI engine-out and tailpipe particulate matter emissions; 2010.

[15] M.D. Hays, W. Preston, B.J. George, J. Schmid, R. Baldauf, R. Snow, et al., Carbonaceous aerosols emitted from light-duty vehicles operating on gasoline and ethanol fuel blends, *Environ Sci Technol* **47** (24), 2013, 14502–14509.

[16] M.M. Maricq, J.J. Szente and K. Jahr, The impact of ethanol fuel blends on pm emissions from a light-duty GDI vehicle, *Aerosol Sci Technol* **46** (5), 2012, 576–583.

[17] M. Clairotte, T.W. Adam, A.A. Zardini, U. Manfredi, G. Martini, A. Krasenbrink, et al., Effects of low temperature on the cold start gaseous emissions from light duty vehicles fuelled by ethanol-blended gasoline, *Appl Energy* **102**, 2013, 44–54.

[18] Council Directive 70/220/EEC of 20 March 1970 on the approximation of the laws of the Member States relating to measures to be taken against air pollution by gases from positive-ignition engines of motor vehicles.

[19] J. Grabowsky, T. Streibel, M. Sklorz, J.C. Chow, J.G. Watson, A. Mamakos, et al., Hyphenation of a carbon analyzer to photo-ionization mass spectrometry to unravel the organic composition of particulate matter on a molecular level, *Anal Bioanal Chem* **401** (10), 2011, 3153–3164.

[20] J. Diab, T. Streibel, F. Cavalli, S.C. Lee, H. Saathoff, A. Mamakos, et al., Hyphenation of a EC/OC thermal-optical carbon analyzer to photo-ionization time-of-flight mass spectrometry: an off-line aerosol mass spectrometric approach for characterization of primary and secondary particulate matter, *Atmos Meas Tech* **8** (8), 2015, 3337–3353.

[21] T.W. Adam, M. Clairotte, T. Streibel, M. Elsasser, A. Pommeres, U. Manfredi, et al., Real-time analysis of aromatics in combustion engine exhaust by resonance-enhanced multiphoton ionisation time-of-flight mass spectrometry (REMPI-TOF-MS): a robust tool for chassis dynamometer testing, *Anal Bioanal Chem* **404** (1), 2012, 273–276.

[22] T.W. Adam, R. Chirico, M. Clairotte, M. Elsasser, U. Manfredi, G. Martini, et al., Application of modern online instrumentation for chemical analysis of gas and particulate phases of exhaust at the European Commission heavy-duty vehicle emission laboratory, *Anal Chem* **83** (1), 2011, 67–76.

[23] J.C. Chow, J.G. Watson, L.-W.A. Chen, M.O. Chang, N.F. Robinson, D. Trimble, et al., The IMPROVE_A temperature protocol for thermal/optical carbon analysis: maintaining consistency with a long-term database, *J Air*

Waste Manage Assoc **57** (9), 2007, 1014–1023.

[24] U. Boesl, R. Weinkauf, C. Weickhardt and E.W. Schlag, Laser ion sources for time-of-flight mass spectrometry, *Int J Mass Spectrom Ion Processes* **131**, 1994, 87–124.

[25] T. Streibel, F. Mühlberger, R. Geißler, M. Saraji-Bozorgzad, T. Adam and R. Zimmermann, Influence of sulphur addition on emissions of polycyclic aromatic hydrocarbons during biomass combustion, *Proc Combust Inst* **3** (2), 2015, 1771–1777.

[26] M. Munoz, N.V. Heeb, R. Haag, P. Honegger, K. Zeyer, J. Mohn, et al., Bioethanol blending reduces nanoparticle, PAH, and Alkyl- and nitro-PAH emissions and the genotoxic potential of exhaust from a gasoline direct injection flex-fuel vehicle, *Environ Sci Technol* **50** (21), 2016, 11853–11861.

[27] J. Schnelle-Kreis, J. Orasche, G. Abbaszade, K. Schafer, D.P. Harlos, A.D.A. Hansen, et al., Application of direct thermal desorption gas chromatography time-of-flight mass spectrometry for determination of nonpolar organics in low-volume samples from ambient particulate matter and personal samplers, *Anal Bioanal Chem* **401** (10), 2011, 3083–3094.

[28] J. Watson, Differences in the carbon composition of source profiles for diesel- and gasoline-powered vehicles, *Atmos Environ* **28** (15), 1994, 2493–2505.

[29] A. Fushimi, Y. Kondo, S. Kobayashi, Y. Fujitani, K. Saitoh, A. Takami, et al., Chemical composition and source of fine and nanoparticles from recent direct injection gasoline passenger cars: effects of fuel and ambient temperature, *Atmos Environ* **124**, 2016, 77–84.

[30] J. Wu, K.H. Song, T. Litzinger, S.-Y. Lee, R. Santoro, M. Linevsky, et al., Reduction of PAH and soot in premixed ethylene-air flames by addition of ethanol, *Combust Flame* **144** (4), 2006, 675–687.

[31] C. Gehm, T. Streibel, J. Passig and R. Zimmermann, Determination of relative ionization cross sections for resonance enhanced multiphoton ionization of polycyclic aromatic hydrocarbons, *Appl Sci* **8** (9), 2018, 1617.

[32] M. Frenklach, Reaction mechanism of soot formation in flames, *PCCP* **4** (11), 2002, 2028–2037.

[33] A. Fushimi, K. Saitoh, Y. Fujitani, S. Hasegawa, K. Takahashi, K. Tanabe, et al., Organic-rich nanoparticles (diameter: 10–30 nm) in diesel exhaust: fuel and oil contribution based on chemical composition, *Atmos Environ* **45** (35), 2011, 6326–6336.

[34] E. Schmider, M. Ziegler, E. Danay, L. Beyer and M. Bühner, Is it really robust?, *Methodology* **6** (4), 2010, 147–151.

[35] Y. Zhi, R. Zong, L. Guangxuan, H. Liu and T. Jialei, The source identification and classification study of soot after combustion, *Fire Mater* **37** (3), 2013, 246–256.

[36] P.K. Kanaujia, D. Singh, D. Tripathi, L.N.S.K. Konathala, S. Saran, R.K. Chauhan, et al., Characterization and identification of polycyclic aromatic hydrocarbons in diesel particulate matter, *Anal Lett* **48** (14), 2015, 2303–2318.

[37] J.J. Schauer, M.J. Kleeman, G.R. Cass and Bernd R.T. Simoneit, Measurement of emissions from air pollution sources. 5. C 1−C 32 organic compounds from gasoline-powered motor vehicles, *Environ Sci Technol* **36** (6), 2002, 1169–1180.

[38] N.M. Donahue, A.L. Robinson, C.O. Stanier and S.N. Pandis, Coupled partitioning, dilution, and chemical aging of semivolatile organics, *Environ Sci Technol* **40** (8), 2006, 2635–2643.

[39] I.J. Keyte, R.M. Harrison and G. Lammel, Chemical reactivity and long-range transport potential of polycyclic aromatic hydrocarbons – a review, *Chem Soc Rev* **42** (24), 2013, 9333–9391.

[40] H.-R. Paur, F.R. Cassee, J. Teeguarden, H. Fissan, S. Diabate, M. Aufderheide, et al., In-vitro cell exposure studies for the assessment of nanoparticle toxicity in the lung—a dialog between aerosol science and biology, *J Aerosol Sci* **42** (10), 2011, 668–692.

[41] S. Oeder, T. Kanashova, O. Sippula, S.C. Sapcariu, T. Streibel, J.M. Arteaga-Salas, et al., Particulate matter from both heavy fuel oil and diesel fuel shipping emissions show strong biological effects on human lung cells a realistic and comparable in vitro exposure conditions, *PLoS ONE* **10** (6), 2015, e0126536.

Appendix A. Supplementary data

The following are the Supplementary data to this article:

Multimedia Component 1

Supplementary data 1

Graphical abstract

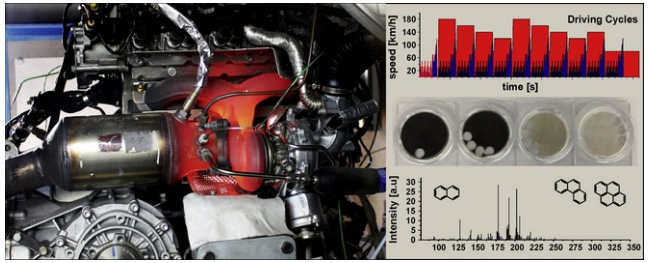

Highlights

- High velocity conditions with increased concentrations for particulate constituents.
- Strong decreased PM emissions by usage of E85.
- Driving cycle affects quantitative emissions, but not the molecular pattern.
- Simultaneous quantification of EC, OC and three PAHs.

Queries and Answers

Query: Your article is registered as a regular item and is being processed for inclusion in a regular issue of the journal. If this is NOT correct and your article belongs to a Special Issue/Collection please contact r.shivaram@elsevier.com immediately prior to returning your corrections.
Answer: Yes

Query: The author names have been tagged as given names and surnames (surnames are highlighted in teal color). Please confirm if they have been identified correctly.
Answer: Yes

Query: Please check the edit made in the affiliation “a and b”, and correct if necessary.
Answer: Yes

Query: Have we correctly interpreted the following funding source(s) and country names you cited in your article: Deutsche Forschungsgemeinschaft, Germany? Helmholtz Association, Germany? /
Answer: Yes